Differential DNA Methylation and Expression of miRNAs in Adipose Tissue From Twin Pairs Discordant for Type 2 Diabetes

Emma Nilsson,[1] Magdalena Vavakova,[1,2] Alexander Perfilyev,[1] Johanna Säll,[1] Per-Anders Jansson,[3] Pernille Poulsen,[4] Jonathan Lou S. Esguerra,[5] Lena Eliasson,[5] Allan Vaag,[6] Olga Göransson,[2] and Charlotte Ling[1]

Diabetes 2021;70:2402–2418 | https://doi.org/10.2337/db20-0324

The prevalence of type 2 diabetes (T2D) is increasing worldwide, but current treatments have limitations. miRNAs may play a key role in the development of T2D and can be targets for novel therapies. Here, we examined whether T2D is associated with altered expression and DNA methylation of miRNAs using adipose tissue from 14 monozygotic twin pairs discordant for T2D. Four members each of the miR-30 and let-7-families were downregulated in adipose tissue of subjects with T2D versus control subjects, which was confirmed in an independent T2D case-control cohort. Further, DNA methylation of five CpG sites annotated to gene promoters of differentially expressed miRNAs, including miR-30a and let-7a-3, was increased in T2D versus control subjects. Luciferase experiments showed that increased DNA methylation of the *miR-30a* promoter reduced its transcription in vitro. Silencing of miR-30 in adipocytes resulted in reduced glucose uptake and TBC1D4 phosphorylation; downregulation of genes involved in demethylation and carbohydrate/lipid/amino acid metabolism; and upregulation of immune system genes. In conclusion, T2D is associated with differential DNA methylation and expression of miRNAs in adipose tissue. Downregulation of the miR-30 family may lead to reduced glucose uptake and altered expression of key genes associated with T2D.

In subjects with type 2 diabetes (T2D), the adipose tissue function is frequently disturbed by insulin resistance, leading to impaired glucose uptake, dysregulation of adipokines, and impaired suppression of lipolysis. This results in elevated lipid levels in circulation and storage of fat in other tissues such as muscle, liver, and pancreas (1). Even though insulin-stimulated glucose disposal in adipose tissue accounts for <5% of an oral glucose load (2), selective *GLUT4* knockdown (KD) in adipose tissue causes insulin resistance in muscle and liver (3).

miRNAs are small noncoding RNA molecules that regulate expression and, consequently, many physiological processes. In adipose tissue, miRNAs regulate adipogenesis and specific endocrine/metabolic functions (4,5). For example, some miRNAs control differentiation of adipocytes by regulating the Wnt/β-catenin signaling pathway (5), regulate insulin sensitivity of adipocytes via the PTEN/PI3K/AKT pathway (6), and regulate oxidative catabolism of fatty acids via PPARα (7). However, it is less clear which miRNAs might be involved in T2D pathology in human adipose tissue in vivo.

DNA methylation of miRNA promoters can inhibit transcription of miRNAs (8). Indeed, epigenetic regulation of miRNA levels have been described in several pathophysiological processes (9,10). For instance, transcrip-

[1]Epigenetics and Diabetes Unit, Department of Clinical Sciences, Lund University Diabetes Centre, Lund University, Scania University Hospital, Malmö, Sweden
[2]Diabetes, Metabolism and Endocrinology, Department of Experimental Medical Science, Lund University, Lund, Sweden
[3]Wallenberg Laboratory, Sahlgrenska University Hospital, Gothenburg, Sweden
[4]Global Development, Novo Nordisk A/S, Søborg, Denmark
[5]Islet Cell Exocytosis Unit, Department of Clinical Sciences, Lund University Diabetes Centre, Lund University, Malmö, Sweden
[6]Steno Diabetes Center Copenhagen, Gentofte, Denmark

Corresponding author: Emma Nilsson, emma_a.nilsson@med.lu.se

Received 3 April 2020 and accepted 21 July 2021

This article contains supplementary material online at https://doi.org/10.2337/figshare.15036348.

E.N. and M.V. contributed equally to this study.

tional silencing by hypermethylation causes the loss of tumor-suppressor miRNAs in cancer (11,12). Programmed epigenetic changes in miRNAs may also contribute to the link between early-life nutrition and long-term risk of metabolic disease (13). Nevertheless, it is not well established whether such epigenetic changes are responsible for impaired adipose tissue function in T2D.

miRNAs may provide attractive therapeutic targets for T2D because of their involvement in insulin secretion (14) and insulin sensitivity (15). Some studies have investigated the role of miRNAs in human adipose tissue in relation to insulin resistance (16). For instance, eleven miRNAs displayed differential expression in adipose tissue from obese insulin-resistant compared with obese insulin-sensitive women (17), and another study suggested that miR-103 affects the development of adiposity and glucose metabolism (18). However, there is still a lack of detailed knowledge of miRNA regulation of T2D pathologies in human adipose tissue.

In the current study, we aimed to identify differentially expressed miRNAs and epigenetic regulation of their expression in T2D using adipose tissue from a unique human cohort of monozygotic (MZ) twin pairs discordant for T2D. We further explored whether identified miRNAs affect phenotypes related to T2D in adipocytes cultured in vitro. The genomic identity of MZ twins provides a powerful design for detection of differentially expressed miRNAs (19) and acquired DNA methylation changes in miRNA genes related to T2D. The fact that twins provide naturally matched pairs reduces the effects of possible confounders such as genetics, age, and sex. We successfully identified differentially expressed miRNAs in adipose tissue from the twins and inferred that the differences in expression are associated with differential DNA methylation of miRNA promoters. We validated these findings in an independent T2D case-control cohort. Silencing of the most promising candidate miRNAs in adipocytes demonstrated their effects on glucose uptake, insulin signaling, and regulation of T2D pathology–related genes.

RESEARCH DESIGN AND METHODS

Study Participants and Clinical Examination

Fourteen MZ twin pairs discordant for T2D recruited through Scandinavian twin registries were included in the study (nine Swedish and five Danish twin pairs). Zygosity was confirmed by analysis of 730,525 genetic markers using HumanOmniExpress arrays (Illumina, San Diego, CA). Further, 28 normal glucose tolerant (NGT) and 28 T2D unrelated subjects, pairwise matched for age and sex, and with no difference in BMI between the groups, were selected from a larger twin cohort (20) and included for biological validation as a case-control cohort. After an overnight fast, subcutaneous adipose tissue biopsies were obtained under local anesthesia, frozen in liquid nitrogen, and stored at −80°C. Clinical characteristics of both cohorts are described in Table 1 and have previously been published (21). Glucose tolerance was measured with a 75-g oral glucose tolerance test, with T2D determined according to the 1999 World Health Organization criteria. All study participants gave informed consent. The study was carried out in accordance with the Declaration of Helsinki.

RNA Extraction

Total RNA was extracted with the miRNeasy kit (QIAGEN, Hilden, Germany). RNA quantity and purity were determined spectrophotometrically (NanoDrop Technologies, Wilmington, DE). RNA integrity was determined with the Experion system (Bio-Rad Laboratories, Hercules, CA).

Table 1—Clinical characteristics of study subjects in the T2D discordant twin cohort and in the T2D case-control cohort for validation

	Discordant twins		Case-control cohort	
	No diabetes	T2D	NGT	T2D
N (male/female)	14 (9/5)	14 (9/5)	28 (15/13)	28 (15/13)
Age (years)	67.6 ± 7.7	67.6 ± 7.7	74.3 ± 4.3	74.5 ± 4.2
BMI (kg/m^2)	29.8 ± 6.8	32.0 ± 7.1*	27.0 ± 3.6	27.4 ± 3.6
Fat% (n = 9 pairs)	30.5 ± 8.8	33.6 ± 9.4*		
Fasting plasma glucose (mmol/L)	6.0 ± 0.5	9.3 ± 2.6#	5.5 ± 0.5	7.1 ± 1.9#
2-h glucose (mmol/L)	8.3 ± 1.8	16.1 ± 5.2*	6.6 ± 0.7	15.1 ± 5.0#
HbA_{1c} (%)	5.9 ± 0.4	7.5 ± 1.8*	5.7 ± 0.3	6.6 ± 1.3#
HbA_{1c} (mmol/mol)	41.0 ± 4.4	58.0 ± 19.7*	39.0 ± 3.3	49.0 ± 14.0#

Data are means ± SD unless otherwise indicated. Among the discordant twins, the cotwin without diabetes exhibited NGT in 4 pairs and impaired glucose tolerance in 10 pairs. Among the discordant twins, one of the twins with T2D and two of the twins without diabetes were smoking (data available for nine twin pairs). Average duration of T2D among discordant twins was 11.3 ± 3.7 years (data available for six subjects). *$P < 0.05$ and #$P < 0.001$, subjects with T2D vs. subjects without diabetes or NGT subjects.

miRNA Expression Arrays

miRNA expression was analyzed in adipose tissue from 12 of the 14 discordant twin pairs with miRNA 3.0 arrays (Affymetrix, Santa Clara, CA) according to the manufacturer's recommendations. Robust multichip average (RMA) expression measures were computed with the oligo package in Bioconductor (release 3.10) (22). Since not all of 1,733 miRNAs included in the array are expressed in adipose tissue, the analysis was restricted to 408 miRNAs known to be expressed in adipose tissue, as determined by either of two studies (23,24). Comparisons between discordant twins were based on paired two-tailed Wilcoxon statistics. Intra–twin pair correlations of within–twin pair differences in MZ twins were analyzed using Spearman statistics.

Quantification of miRNA Levels in Adipose Tissue and Adipocytes

RNA was amplified and reverse transcribed to cDNA with TaqMan PreAmp Master Mix and MicroRNA Reverse Transcription Kit (Thermo Fisher Scientific, Rockford, IL). miRNA expression was quantified with specific TaqMan miRNA assays (hsa-miR-30a-5p, assay 000417; hsa-miR-30b, assay 000602; hsa-miR-30c, assay 000419; hsa-miR-30d, assay 000420; hsa-let-7a, assay 000377; hsa-let-7b, assay 002619; hsa-let-7f, assay 000382; and hsa-let-7g, assay 002282; all Thermo Fisher Scientific) and normalized to RNU48 expression (human, assay 001006; Thermo Fisher Scientific) or snoRNA202 (mouse, assay 001232; Thermo Fisher Scientific). miRNA levels were quantified with the QuantStudio 7 Flex Real-Time PCR System (Applied Biosystems, Foster City, CA). Validation of miRNA expression differences between subjects with and without T2D were based on one-tailed Mann-Whitney statistics.

3T3-L1 Cell Culture, Differentiation, and Silencing Experiments

3T3-L1 murine fibroblasts were cultured in DMEM (25 mmol/L glucose; Thermo Fisher Scientific) supplemented with 10% FBS (Thermo Fisher Scientific) and 100 units/mL penicillin/streptomycin (Thermo Fisher Scientific) in 5% CO_2 humidified atmosphere at 37°C. For differentiation to adipocyte-like cells, 2-day postconfluent cells were incubated with 1 μmol/L dexamethasone (Sigma-Aldrich, St Louis, MO), 0.5 mmol/L 3-isobutyl-1-methylxantine (Sigma-Aldrich), and 1.74 μmol/L insulin (Sigma-Aldrich) for 72 h and then cultivated in DMEM media. The differentiation rate was typically 80–90%.

Nine days postdifferentiation, cells were separately transfected with 100 nmol miRCURY LNA inhibitors (mmu-miR-30a-5p, mmu-miR-30b-5p, and mmu-miR-30c-5p or mmu-miR-30d-5p, respectively; QIAGEN) or with 100 nmol of negative control (NC) siRNA (Negative control A, miRCURY LNA miRNA Inhibitor Control; QI AGEN) using Lipofectamine 2000 transfection reagent (Thermo Fisher Scientific), according to the manufacturer's instructions. Cells were then incubated for 48 h and RNA was isolated using miRNeasy kit (QIAGEN). Unspecific downregulation of miR-30d by silencing of miR-30a and unspecific downregulation of miR-30b by silencing of miR-30c, and vice versa, were observed (Supplementary Fig. 1). Sequence analysis of the miR-30 family revealed 100% identity between human and mouse miR-30a, b, c, d, and e and a great similarity between miR-30a and miR-30d (1 nucleotide [nt] substitution), miR-30a and miR-30e (1 nt substitution) and miR-30c and miR-30b (2 nt deletions) that could explain the unspecific silencing (Supplementary Fig. 2). Therefore, 3T3-L1 adipocytes were cotransfected with miR-30a and miR-30c inhibitors (100 nmol in total) for complete miR-30a, b, c, and d silencing ($n = 6$).

RNA (six independent passages) was used for mRNA microarray analysis with Clariom S Assay (902930; Thermo Fisher Scientific), according to the manufacturer's instructions. Preprocessing was performed with RMA using the Expression Console v1.4.1.46 software (Thermo Fisher Scientific). Data were log2 transformed and analyzed with the limma package in Bioconductor (release 3.10) (25). Data are presented as log2 fold change (log2 FC) between mmu-miR-30a+c silencing and NC. Data were analyzed by paired t test, and P values were adjusted with the use of Benjamini-Hochberg false discovery rate (FDR) analysis. FDR <5% ($q < 0.05$) was considered significant.

Microarray data were analyzed by gene set enrichment analysis (GSEA) using Reactome pathways (26) and Kyoto Encyclopedia of Genes and Genomes (KEGG) pathways (www.kegg.jp) available from fgsea package and reactome.db (Bioconductor, release 3.10).

Luciferase Assay

A total of 1,500 base pairs (bp) DNA fragments of *hsa-miR-30a* (GRCh38.p13, chromosome 6 [chr6]: 71403621–71405121) and *hsa-let-7a-3* (GRCh38.p13, chr22: 46110248–46112748) promoter regions were synthetized and inserted into a CpG-free firefly luciferase reporter vector (pCpGL-basic; GenScript, Piscataway, NJ). The construct was then methylated using SssI methyltransferase with *S*-adenosylmethionine as a methyl donor (B9003S; New England Biolabs, Cambridge, MA). The *hsa-miR-30a* and *hsa-let-7a-3* promoter sequences contain 10 and 59 SssI target sites, respectively. Nonmethylated constructs were used as a background control. Nondifferentiated 3T3-L1 cells were seeded into a 96-well plate and cotransfected with the methylated or nonmethylated construct, and the pRL *Renilla* luciferase control-reporter vector (pRL-CMV vector; Promega, Madison, WI), using FuGENE HD Transfection Reagent (E2311; Promega), according to the manufacturer's instructions. Cells were lysed after 48 h, and the firefly and *Renilla* luciferase activity was measured with the Dual-Luciferase Reporter Assay system (E1910; Promega) in six independent passages. Firefly luciferase activity was normalized to *Renilla* luciferase activity and corrected for background value. Paired t test was used to determine

differences in the transcriptional activity of unmethylated and methylated vectors.

Glucose Uptake in 3T3-L1 Adipocytes

3T3-L1 adipocytes were cotransfected with miR-30a and miR-30c inhibitors or NC siRNA for 45 h, starved in Krebs-Ringer bicarbonate HEPES buffer (0.75 mmol/L $CaCl_2$ * 2 H_2O, 120 mmol/L NaCl, 4 mmol/L KH_2PO_4, 1 mmol/L $MgSO_4$ * 7 H_2O, 10 mmol/L $NaHCO_3$, and 30 mmol/L HEPES [pH 7.4]) for 2 h, and incubated with or without insulin (0 nmol/L [basal], 1.7 nmol/L, and 100 nmol/L insulin; Novo Nordisk, Bagsværd, Denmark) or cytochalasin B (10 μmol/L, Sigma-Aldrich) for 30 min. Glucose uptake was determined as previously described (27). Experiments were performed on five independent passages and in triplicates. Cytochalasin B values were subtracted, and results were normalized to protein concentrations measured with a Bradford protein assay and NC basal values (28). Paired *t* tests were used to determine differences between glucose uptake of mmu-miR-30a+c KD and NC cells.

Insulin Stimulation of 3T3-L1 Adipocytes

Differentiated 3T3-L1 adipocytes (day 9) were cotransfected with miR-30a and miR-30c for 48 h as previously described and stimulated with or without 1 nmol/L insulin (Novo Nordisk) for 15 min. Protein samples were collected by lysis in cOmplete Protease Inhibitor Cocktail (1 tablet/50 mL), 1 mmol/L dithiothreitol, 1 mmol/L EDTA, 1 mmol/L EGTA, 5 mmol/L Na-pyrophosphate, 0.27 mol/L sucrose, 50 mmol/L NaF, 50 mmol/L Tris-Base, 1 mmol/L Na-orthovanadate, and 1% NP40, and their concentrations were measured with Bradford assay. Paired *t* tests were used to determine differences between KD and NC.

Western Blot Analysis

Western blot was performed using the following primary antibodies: AGPAT9 (GPAT3, HPA029414; Atlas Antibodies, Bromma, Sweden), AS160 (TBC1D4, 07-741; Sigma-Aldrich), phosphorylated AS160 T642 (TBC1D4, 44-1071G; MyBioSource, San Diego, CA), PKB (AKT1, 9272; Cell Signaling Technology, Danvers, MA), phosphorylated PKB S473 (AKT1, 44621G; Thermo Fisher Scientific), ELOVL6 (PA5-13455; Thermo Fisher Scientific), and HSP90 (610418; BD Biosciences, Franklin Lakes, NJ). GLUT1 antibody was kindly provided by Samuel W. Cushman (National Institutes of Health).

For Western blot analysis in cultured adipocytes, cell lysates containing LDS sample buffer (Thermo Fisher Scientific) were heated for 5 min in 95°C and loaded on precast Novex Bis-Tris 4–12% polyacrylamide gels (Thermo Fisher Scientific). Proteins were transferred to nitrocellulose membrane (Amersham Protran Western blotting membrane; Sigma-Aldrich) and blocked for 1 h in 10% milk in TBS-T (Tris-buffered saline, pH 7.6, and 0.1% Tween 20; Sigma-Aldrich). Membranes were incubated overnight in primary antibodies at 4°C diluted in TBS-T with 5% BSA (Sigma-Aldrich). After incubation in mouse or rabbit secondary antibody (NA931, Sigma-Aldrich, and A16096, Thermo Fisher Scientific), signals were visualized with ECL (SuperSignal West Pico and Femto Chemiluminescent Substrates; Thermo Fisher Scientific) and detected with a Bio-Rad ChemiDoc CCD camera and the Image Lab software (Bio-Rad Laboratories). Signals were quantified and normalized to HSP90.

Human adipose tissue biopsies were lysed in ice-cold radioimmunoprecipitation assay buffer (50 mmol/L Tris-HCl, pH 7.5; 150 mmol/L NaCl; 2 mmol/L EDTA; 1% Triton X-100; 0.5% Na-deoxycholate; and 0.1% SDS) containing cOmplete Protease Inhibitor Cocktail (1 tablet per 50 mL; Roche). Biopsies were homogenized in a TissueLyser II (QIAGEN). Protein concentrations were determined with the BCA method (Pierce BCA Protein Assay Kit; Thermo Fisher Scientific).

Total protein (5 μg) was mixed with sample buffer (60 mmol/L Tris-HCl, pH 6.8; 2% [w/v] SDS; 10% [v/v] glycerol; 2% [v/v] 2-mercaptoethanol), separated with gel electrophoresis (Criterion TGX Stain-Free Precast Gradient Gels; Bio-Rad Laboratories) and transferred to Low Fluorescence PVDF Membranes (0.45 μm; Bio-Rad Laboratories). Membranes were blocked in 5% (w/v) milk in TBS-T (0.05% [w/v] Tween-20), incubated with primary antibody diluted in 5% (w/v) BSA (HyClone; Cytiva) in TBS-T overnight at +4°C and horseradish peroxidase-conjugated secondary antibody (goat anti-rabbit IgG, RRID:AB_2099233; Cell Signaling Technology) for 1 h in room temperature. Proteins were detected with enhanced chemiluminescence (SuperSignal West Femto) in a ChemiDoc MP (Bio-Rad Laboratories) and quantified based on total protein normalization with stain-free gels in Image Lab version 6.1.0 (Bio-Rad V3 Western Workflow; Bio-Rad Laboratories).

SGBS Cell Culture, Differentiation, and Silencing Experiments

Simpson-Golabi-Behemil syndrome (SGBS) cells were cultured and differentiated into mature adipocytes as previously described (29). Cells were used at day 9 with the differentiation rate 70–80% (Supplementary Fig. 3). Silencing was performed under the same experimental conditions and with the use of the same inhibitors for miR-30a, miR-30c, and NC as in 3T3-L1, due to 100% similarity between these human and mouse miRNAs. Cells were collected after 48 h, RNA was extracted and reverse transcribed, and efficiency of KD was determined (Supplementary Fig. 4).

RNA was extracted from miR-30a+c KD and NC SGBS adipocytes (five independent passages) and used for mRNA microarray analysis with Clariom S human arrays (Thermo Fisher Scientific) according to the manufacturer's instructions. Array quality control, data normalization (Signal Space Transformation (SST)-RMA), and log2 transformation were performed with Transcriptome Analysis Console (TAC)

Software (Thermo Fisher Scientific). Data were analyzed with eBayes ANOVA between KD and NC, calculated as condition (KD vs. NC) + repeated measures (passages). FDR <5% ($q < 0.05$) was considered significant.

We applied GSEA (30) to expression array data using KEGG pathways. Probes corresponding to transcripts were used and ranked according to the fold change.

Data and Resource Availability

The data sets generated in the course of the current study are available from the corresponding author upon reasonable request. No applicable resources were generated or analyzed during the current study.

RESULTS

Specific miRNAs Are Differentially Expressed in Adipose Tissue of T2D Subjects

We first analyzed expression of 408 miRNAs in adipose tissue from 12 MZ twin pairs discordant for T2D (Table 1). Thirty miRNAs (7.4% of those analyzed) were differentially expressed in the twin pairs ($P < 0.05$) (Table 2), which is more than expected by chance ($P < 0.05$, χ^2 test). The expression of the vast majority of the identified miRNAs (25 [83%]) was lower in the T2D than in non-T2D adipose tissue. Since miRNAs within the same family often target the same mRNAs, we asked whether the differentially expressed miRNAs in discordant twins represented the same family (or families), as defined by miRBase (release 22.1) (31). Indeed, three miRNA families were represented by at least two differentially expressed miRNAs (Table 2). The hsa-miR-30 and hsa-let-7 families, with 5 and 13 family members, respectively, were overrepresented among the dysregulated miRNAs, with 4 family members each downregulated in T2D twins (Fig. 1*A*). Further, intra–twin pair correlations revealed that the differences in log2 expression levels of 4 of the 30 identified dysregulated miRNAs (miR-128, miR-151b, miR-26b, and miR-30b) correlated with differences in fasting glucose levels ($\rho = 0.61$–0.67, $P < 0.05$) (Supplementary Table 1).

To test the robustness of the above observations, we next investigated the expression of hsa-miR-30a–d and hsa-let-7a, b, f, and g in adipose tissue from NGT and T2D unrelated subjects (Table 1). All miRNAs tested followed the same pattern as in T2D discordant twins, with reduced levels in adipose tissue of T2D subjects compared with that of control subjects (Fig. 1*B*) (all $P \leq 0.05$, except for miR-30d [$P = 0.1$]).

Predicted Targets of miRNAs Have Differential mRNA Expression in Human T2D Adipose Tissue

To evaluate the possible functional involvement of these miRNAs in T2D, we next used TargetScan (release 7.2) (32) to predict conserved targets of the differentially expressed miRNAs. We then identified the conserved targets with differential expression in discordant twins, using previously published mRNA data (21) (Supplementary Table 2).

TargetScan predicted 1,576 conserved targets for the human miR-30 family; 285 of these exhibited differential expression in adipose tissue from the T2D discordant twins ($P < 0.05$) (Supplementary Table 2). The identified targets participate in pathways related to, e.g., membrane transport, amino acid metabolism, and development and regeneration (Supplementary Fig. 5). The targets included *ELOVL6* and *B4GALT6*, two genes with the largest expression difference in adipose tissue of T2D twins versus twins without diabetes (21). Since ELOVL6 and B4GALT6 are important for lipid metabolic processes, we next analyzed the relationship between expression of hsa-miR-30a–d and *ELOVL6* and *B4GALT6*, focusing on intra–twin pair correlations in the MZ twins. We observed significant intra–twin pair correlations between differences in *ELOVL6* mRNA and differences in hsa-miR-30a levels, miR-30b levels, and miR-30c levels (Fig. 1*C*–*E*). Moreover, differences in *B4GALT6* mRNA and differences in hsa-miR-30d levels were also significantly correlated (Fig. 1*F*).

Further TargetScan analysis predicted 1,207 conserved targets for the human let-7 family; 210 of these were differentially expressed in adipose tissue from T2D discordant twins (Supplementary Table 2). The predicted differentially expressed let-7 target genes are involved in pathways associated with, e.g., metabolism of terpenoids and polyketides, aging, and cancer (Supplementary Fig. 6). One target was *AGPAT9*, one of the genes with the largest expression difference in adipose tissue from T2D twins versus twins without diabetes (21). The difference in *AGPAT9* expression between co-twins was significantly correlated in intra–twin pair analysis with the difference in hsa-let-7a levels (Fig. 1*G*). We further analyzed adipose tissue AGPAT9 protein levels in 8 T2D subjects and 13 control subjects without diabetes (Supplementary Table 3). There was no difference in protein levels between T2D versus control subjects but a significant negative correlation between AGPAT9 and BMI ($r = -0.51$, $P = 0.02$) (Supplementary Fig. 7*A*), suggesting that AGPAT9 might be related to obesity rather than T2D. Indeed, also let7a ($r = -0.65$, $P = 0.02$), let7b ($r = -0.68$, $P = 0.015$), and *AGPAT9* mRNA ($r = -0.58$, $P = 0.046$) levels correlate negatively with BMI in analysis of the 12 twins without diabetes in the discordant twin cohort (Supplementary Fig. 7*B*–*D*). AGPAT9 is a glycerol-3-phosphate acyltransferase, which catalyzes the initial step of de novo triacylglycerol synthesis.

Differential DNA Methylation of Sites Annotated to Differentially Expressed miRNA Genes

Since miRNA expression could be regulated by methylation, we analyzed DNA methylation of CpG sites annotated to miRNA genes (based on Illumina manifest and genome build 37) in adipose tissue from 14 twin pairs discordant for T2D. In the current study we only assessed DNA methylation of sites annotated to

Table 2—Differentially expressed miRNAs in adipose tissue biopsies from 12 MZ twins with T2D compared with their 12 co-twins without diabetes ($P < 0.05$)

Transcript identifier	miRNA family	Accession no.	Non-T2D	T2D	*P*
hsa-let-7f	let-7	MIMAT0000067	8.97 ± 0.50	8.53 ± 0.61	0.004
hsa-miR-4421		MIMAT0018934	0.73 ± 0.22	0.47 ± 0.19	0.006
hsa-let-7g	let-7	MIMAT0000414	9.26 ± 0.47	8.88 ± 0.49	0.008
hsa-miR-519c-3p		MIMAT0002832	0.56 ± 0.10	0.41 ± 0.15	0.008
hsa-miR-128		MIMAT0000424	4.53 ± 0.52	3.90 ± 1.01	0.010
hsa-miR-181d		MIMAT0002821	3.91 ± 0.78	3.46 ± 0.87	0.010
hsa-miR-29b-2-5p		MIMAT0004515	6.66 ± 0.28	6.37 ± 0.38	0.010
hsa-let-7a	let-7	MIMAT0000062	13.01 ± 0.22	12.78 ± 0.28	0.012
hsa-miR-151-3p		MIMAT0000757	7.78 ± 0.23	7.62 ± 0.24	0.012
hsa-miR-151b		MIMAT0010214	7.53 ± 0.15	7.22 ± 0.34	0.012
hsa-miR-26b		MIMAT0000083	5.19 ± 0.46	4.68 ± 0.68	0.015
hsa-miR-338-5p		MIMAT0004701	1.31 ± 0.52	0.82 ± 0.27	0.015
hsa-miR-331-3p		MIMAT0000760	4.99 ± 0.32	4.59 ± 0.45	0.019
hsa-miR-181a-2-3p		MIMAT0004558	4.18 ± 0.61	3.64 ± 0.74	0.019
hsa-miR-30d	miR-30	MIMAT0000245	8.26 ± 0.23	8.07 ± 0.21	0.028
hsa-miR-29c		MIMAT0000681	4.30 ± 1.23	3.63 ± 1.27	0.028
hsa-miR-504		MIMAT0002875	3.31 ± 0.55	2.90 ± 0.86	0.028
hsa-miR-487b	miR-154	MIMAT0003180	4.36 ± 1.05	3.77 ± 1.34	0.028
hsa-miR-411		MIMAT0003329	1.00 ± 0.41	0.76 ± 0.31	0.028
hsa-miR-2355-3p		MIMAT0017950	0.44 ± 0.16	0.28 ± 0.15	0.028
hsa-miR-30c	miR-30	MIMAT0000244	9.45 ± 0.25	9.13 ± 0.34	0.034
hsa-miR-30b	miR-30	MIMAT0000420	7.49 ± 0.42	7.07 ± 0.67	0.034
hsa-miR-342-3p		MIMAT0000753	9.02 ± 0.38	9.24 ± 0.30	0.034
hsa-miR-30a	miR-30	MIMAT0000087	8.61 ± 0.48	8.20 ± 0.60	0.041
hsa-miR-26a-2-3p		MIMAT0004681	0.40 ± 0.16	0.61 ± 0.29	0.041
hsa-miR-455-3p		MIMAT0004784	7.70 ± 0.49	7.94 ± 0.49	0.041
hsa-miR-374b		MIMAT0004955	1.66 ± 0.49	1.22 ± 0.56	0.041
hsa-miR-1185	miR-154	MIMAT0005798	0.46 ± 0.12	0.62 ± 0.21	0.041
hsa-let-7b	let-7	MIMAT0000063	14.21 ± 0.07	14.14 ± 0.12	0.0499
hsa-miR-518b		MIMAT0002844	0.40 ± 0.12	0.60 ± 0.23	0.0499

Data are log2 transformed expression levels (means ± SD). miR family names from miRBase indicate the relatedness between the miRNAs. Families with more than one member are shown.

miRNA genes; results from the analysis of DNA methylation data not focusing on sites annotated to miRNAs have previously been presented (21). A total of 147 sites, which are included on and could be analyzed with the Illumina Infinium HumanMethylation450 BeadChip, were annotated to the 30 miRNAs with differential expression in discordant twins. Ten of these sites, annotated to nine different miRNAs, exhibited differential methylation between T2D twins and twins without diabetes ($P < 0.05$, 6.8% of analyzed sites) (Table 3). Methylation of the majority of these sites (8 sites [80%]) was increased in T2D twins compared with twins without diabetes.

Next, to test the validity of the methylation differences identified in the discordant twins, we analyzed DNA methylation in adipose tissue from the cohort of unrelated subjects. We analyzed methylation of sites annotated to the 30 differentially expressed miRNAs in the discordant twin cohort, in 28 T2D and 28 non-T2D subjects. We identified 26 differentially methylated sites annotated to 14 miRNAs ($P < 0.05$, 18.1% of 144 analyzed sites) (Table 3), which is more than expected by chance ($P < 0.05$, χ^2 test). Methylation of the majority of the identified sites (23 [88%]) was higher in T2D subjects than in subjects without diabetes. Five of 10 sites with differential methylation in the discordant twins were

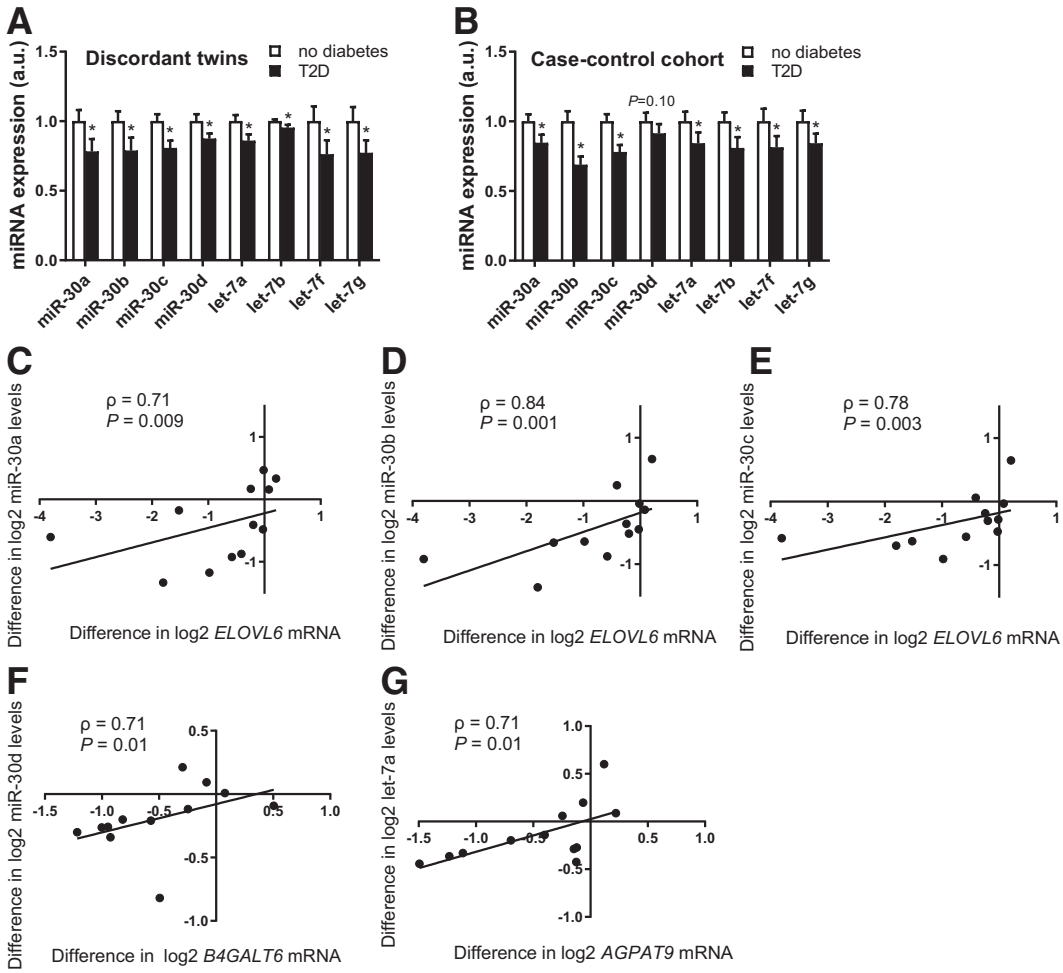

Figure 1—Differentially expressed miRNAs in adipose tissue from T2D subjects and intra–twin pair correlations between differences in specific gene expression and differences in specific miRNA levels. Four members each from the hsa-miR-30 and hsa-let-7 families were downregulated in T2D adipose tissue in the discordant twin cohort (array data, 12 twin pairs) (*A*) and the case-control cohort (quantitative PCR [qPCR] data, 27 subjects without diabetes and 25 T2D subjects) (*B*). Significant intra–twin pair correlations between differences in log2 *ELOVL6* mRNA and log2 hsa-miR-30a levels (*C*), log2 *ELOVL6* mRNA and log2 hsa-miR-30b levels (*D*), log2 *ELOVL6* mRNA and log2 hsa-miR-30c levels (*E*), log2 *B4GALT6* mRNA and log2 hsa-miR-30d levels (*F*), and log2 *AGPAT9* and log2 hsa-let-7a levels (*G*) were observed in 12 discordant twin pairs. In *A* and *B*, data are shown as the mean + SEM, with the mean expression levels for individuals without diabetes set to 1. *$P \leq 0.05$ compared with individuals without diabetes. a.u., arbitrary units. For the miRNA array expression data, while log2 intensity values were used for statistical analyses, non–log-transformed expression values are used in *A*. Within-twin pair differences of the measures were calculated by subtracting the value of the co-twin without diabetes from the value of the T2D co-twin. Intra–-twin pair correlations between within–twin pair differences in MZ twins were analyzed using Spearman statistics.

replicated in this case-control cohort (Table 3), including cg16506910 in the region within 1,500 bp of the transcription start site (TSS1500) of *hsa-miR-30a* and cg26371705 and cg15702185 in TSS1500 of *hsa-let-7a-3* (Fig. 2*A*–*C*).

DNA Methylation Inhibits miRNA Expression In Vitro

Based on the DNA methylation data in the two cohorts, supporting epigenetic regulation of miRNA expression in adipose tissue, we proceeded to test the effects of promoter region methylation of selected miRNA genes on their transcriptional activity. We analyzed methylation of the promoters of *hsa-miR-30a* and *hsa-let-7a-3*, since their methylation was increased and expression decreased in adipose tissue of T2D subjects (Figs. 1*A* and *B* and 2*A*–*C*). Luciferase reporter gene assays revealed that methylation of the proximal promoter region (1,500 bp upstream) of *hsa-miR-30a* significantly suppressed its transcriptional activity compared with unmethylated promoter (Fig. 2*D*). A similar effect was observed for *hsa-let-7a-3*, although it did not reach statistical significance (Fig. 2*E*).

miR-30 Silencing in 3T3-L1 Adipocytes Affects the Transcriptome

To better understand the biological relevance of the identified miRNAs in adipocytes, we tested the effect of silencing specific miRNAs in vitro. We selected the miR-30

Table 3—Differentially methylated sites ($P < 0.05$) in adipose tissue biopsies from 14 MZ twins with T2D compared with their 14 co-twins without diabetes, and a case-control cohort

Target identifier	Gene	Gene region	Non-T2D (mean ± SD), %	T2D (mean ± SD), %	Difference (%-points)	*P*
T2D discordant twins						
cg26371705*	MIRLET7A3, LOC400931	TSS1500, body	70.56 ± 4.53	74.7 ± 4.07	4.13	0.007
cg16506910*	MIR30A	TSS1500	55.12 ± 3.01	57.44 ± 2.21	2.32	0.011
cg22121941	MIRLET7A3, LOC400931, MIRLET7B	TSS200, body, TSS1500	66.45 ± 4.03	68.88 ± 4.41	2.43	0.017
cg03547809*	MIR1185-2, MIR1185-1	TSS1500, TSS200	83.88 ± 2.14	85.04 ± 2.33	1.16	0.020
cg15702185*	MIRLET7A3, LOC400931	TSS1500, body	40.55 ± 4.39	43.65 ± 4.25	3.11	0.030
cg01078903	MIR487B, MIR539	TSS1500, TSS1500	89.68 ± 1.74	88.45 ± 1.52	−1.23	0.030
cg19019198	MIRLET7G, WDR82	TSS200, body	73.16 ± 3.45	75.62 ± 2.64	2.46	0.035
cg01829822*	NCRNA00182, MIR374B, MIR421	Body, TSS200, TSS1500	72.86 ± 5.11	75.87 ± 6.62	3.01	0.035
cg11135080	NFYC, MIR30C1	Body, TSS200	70.09 ± 3.77	72.99 ± 4.29	2.90	0.042
cg01132653	MIR299, MIR411	TSS1500, TSS200	84.77 ± 1.86	83.91 ± 1.83	−0.86	0.049
T2D case-control cohort						
cg22159815	MIR29C	Body	65.9 ± 5.02	60.24 ± 7.79	−5.66	0.0004
cg03446399	MIR29B2	TSS1500	73.68 ± 3.74	76.57 ± 3.24	2.89	0.001
cg19098437	MIR30A	Body	61.83 ± 5.5	65.97 ± 5.53	4.14	0.002
cg03547809*	MIR1185-2, MIR1185-1	TSS1500, TSS200	78.74 ± 2.92	80.36 ± 3.16	1.62	0.006
cg09263904	CTDSP2, MIR26A2	Body, TSS1500	51.02 ± 3.37	53.27 ± 4.14	2.25	0.006
cg01709493	MIR1185-1, MIR1185-2	Body, TSS1500	78.87 ± 2.72	80.92 ± 2.63	2.06	0.007
cg01111856	MIRLET7A3, LOC400931, MIRLET7B	TSS200, body, TSS1500	89.81 ± 7.68	83.37 ± 16.99	–6.44	0.013
cg01190168	CTDSP2, MIR26A2	Body, TSS200	61.57 ± 3.32	63.5 ± 3.9	1.93	0.013
cg08460635	CTDSP1, CTDSP1, MIR26B	Body, body, TSS200	63.64 ± 3.29	65.87 ± 4.88	2.23	0.013
cg11887864	MIR1185-2	TSS200	78.94 ± 2.33	80.28 ± 2.06	1.35	0.014
cg15702185*	MIRLET7A3, LOC400931	TSS1500, Body	31.97 ± 3.86	33.86 ± 2.96	1.89	0.019
cg20815778	MIR30A	TSS200	36.93 ± 5.25	39.83 ± 5.7	2.9	0.02
cg20067612	MIR299, MIR411	TSS1500, TSS1500	71.21 ± 3	72.9 ± 3.04	1.7	0.023
cg00716579	MIR181C, MIR181D	TSS1500, TSS1500	30.75 ± 5.22	33.89 ± 7.25	3.15	0.032
cg11600078	MIR657, AATK, MIR338	TSS1500, body, TSS1500	48.56 ± 4.36	50.97 ± 5.76	2.41	0.034
cg26371705*	MIRLET7A3, LOC400931	TSS1500, body	67.22 ± 5.26	69.3 ± 4.08	2.09	0.034
cg24700993	NFYC, MIR30C1	Body, TSS200	71 ± 3.42	72.54 ± 3.88	1.54	0.038
cg07617764	CTDSP2, MIR26A2	Body, TSS200	59.24 ± 4.01	61.39 ± 5.22	2.15	0.04
cg08695558	MIRLET7A3, LOC400931	TSS1500, body	48 ± 4.79	50.43 ± 5.15	2.43	0.04
cg16506910*	MIR30A	TSS1500	48.55 ± 3.94	50.52 ± 4.05	1.97	0.04
cg01829822*	NCRNA00182, MIR374B, MIR421	Body, TSS200, TSS1500	75.37 ± 8.11	77.01 ± 9.38	1.65	0.043
cg24085713	AATK, MIR338	Body, TSS1500	41.48 ± 4.54	43.51 ± 5.6	2.03	0.043
cg06332842	MIR657, AATK, MIR338	TSS1500, body, TSS1500	75.82 ± 4.35	77.7 ± 4.59	1.88	0.045
cg15851964	CTDSP2, MIR26A2	Body, TSS200	75.61 ± 3.47	77.34 ± 3.59	1.74	0.045
cg04063235	MIRLET7A3, LOC400931, MIRLET7B	TSS200, body, TSS1500	70.25 ± 5.17	72.81 ± 5.23	2.56	0.048
cg06445981	MIR518B	Body	87.09 ± 2.6	85.35 ± 3.47	−1.74	0.048

Sites annotated to miRNAs with differential expression in adipose tissue biopsies from MZ twins with T2D compared with their co-twins without diabetes were included in the analysis. Shown are methylation percentages. The case-control cohort includes 28 T2D and 28 non-T2D subjects. *Differentially methylated in both cohorts.

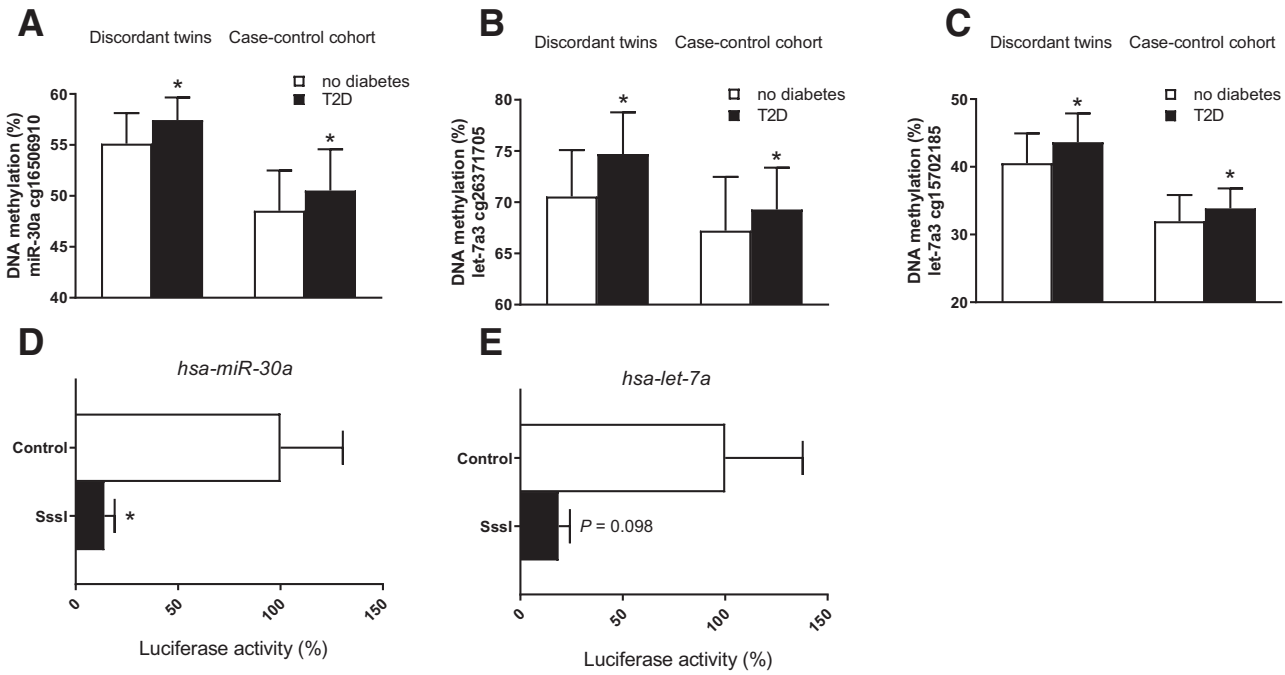

Figure 2—Differentially methylated CpG sites annotated to miRNA genes in adipose tissue from T2D subjects. The methylation of CpG sites cg16506910 in TSS1500 of *hsa-miR-30a* (*A*), and cg26371705 (*B*) and cg15702185 (*C*) in TSS1500 of *hsa-let-7a-3* was increased in adipose tissue from T2D individuals compared with control subjects without diabetes from both the discordant twin cohort (14 twin pairs) and case-control cohort (28 subjects without diabetes and 28 T2D subjects). Reporter gene transcription was determined by measuring luciferase activity (firefly-to-*Renilla* ratio) after SssI in vitro methylation of the *hsa-miR-30a* (*D*) and *hsa-let-7a-3* (*E*) promoters cloned into a CpG-free vector and transfected into nondifferentiated 3T3-L1 cells ($n = 6$). The *hsa-miR-30a* and *hsa-let-7a-3* promoter sequences contain 10 and 59 SssI target sites, respectively. Nonmethylated constructs were used as controls and set to 100%. Data are presented as the mean + SD (*A*–*C*) or mean + SEM (*D* and *E*). *$P < 0.05$.

family for in vitro functional analysis based on the downregulation of four of five family members in adipose tissue of T2D subjects (Fig. 1*A* and *B*) and the identified epigenetic regulation of miR-30a (Fig. 2*A* and *D*). We silenced the expression of mmu-miR-30a, b, c, and d in mature 3T3-L1 adipocytes (Fig. 3*A*). We then analyzed the transcriptome of the silenced cells using microarrays and found 732 significantly downregulated genes ($q < 0.05$) and 246 significantly upregulated genes ($q < 0.05$) in 3T3-L1 adipocytes where mmu-miR-30a, b, c and d had been silenced compared with NC (Supplementary Tables 4 and 5). The 50 genes with the largest expression differences between mmu-miR-30–silenced adipocytes and NC (25 upregulated and 25 downregulated) are shown in Table 4. According to a literature search (articles deposited in the PubMed database prior to 2020) on the relationship of these genes with T2D, diabetes complications, or obesity in human, animal models, or cells, approximately one-third of these top 50 genes are linked with one or more of these search terms, i.e., the gene encoding AMP-activated protein kinase α2 (*Prkaa2/Ampka2*) (Table 4).

We then compared the list of genes with significantly altered expression after mmu-miR-30 silencing (Supplementary Tables 4 and 5) with the differentially expressed genes in adipose tissue from MZ twins discordant for T2D (21). This revealed 17 common genes regulated in the same direction, after conversion of mouse genes to human orthologs, via the biomaRt package (Bioconductor, release 3.10). Two genes (*Ctsz* and *Evc2*) were upregulated and 15 genes were downregulated in both data sets (human T2D adipose tissue and 3T3-L1 miR-30 KD) (Fig. 3*B*). *Ctsz*, encoding cathepsin Z, has been associated with inflammatory conditions in different tissues and has been proposed to be used as a clinical marker for systemic inflammation in humans (33). The downregulated genes were associated with signal transduction (*Braf*) or lipid, amino acid, and carbohydrate metabolism (*Hadh*, *Acat1*, *Aldh6a1*, and *Hibch*). Interestingly, *Tet1*, encoding CpG demethylase, an enzyme involved in regulation of DNA methylation, was downregulated in both human T2D adipose tissue and 3T3-L1 miR-30 KD adipocytes and is a conserved predicted target of the miR-30 family.

We next used GSEA to identify sets of biologically related genes that are altered in the miR-30–silenced adipocytes. Pathway analysis revealed 41 significantly upregulated gene sets and 15 significantly downregulated gene sets ($q < 0.05$) (Supplementary Table 6). The upregulated pathways included gene sets involved in regulation of translation, metabolism of RNA, and the immune system

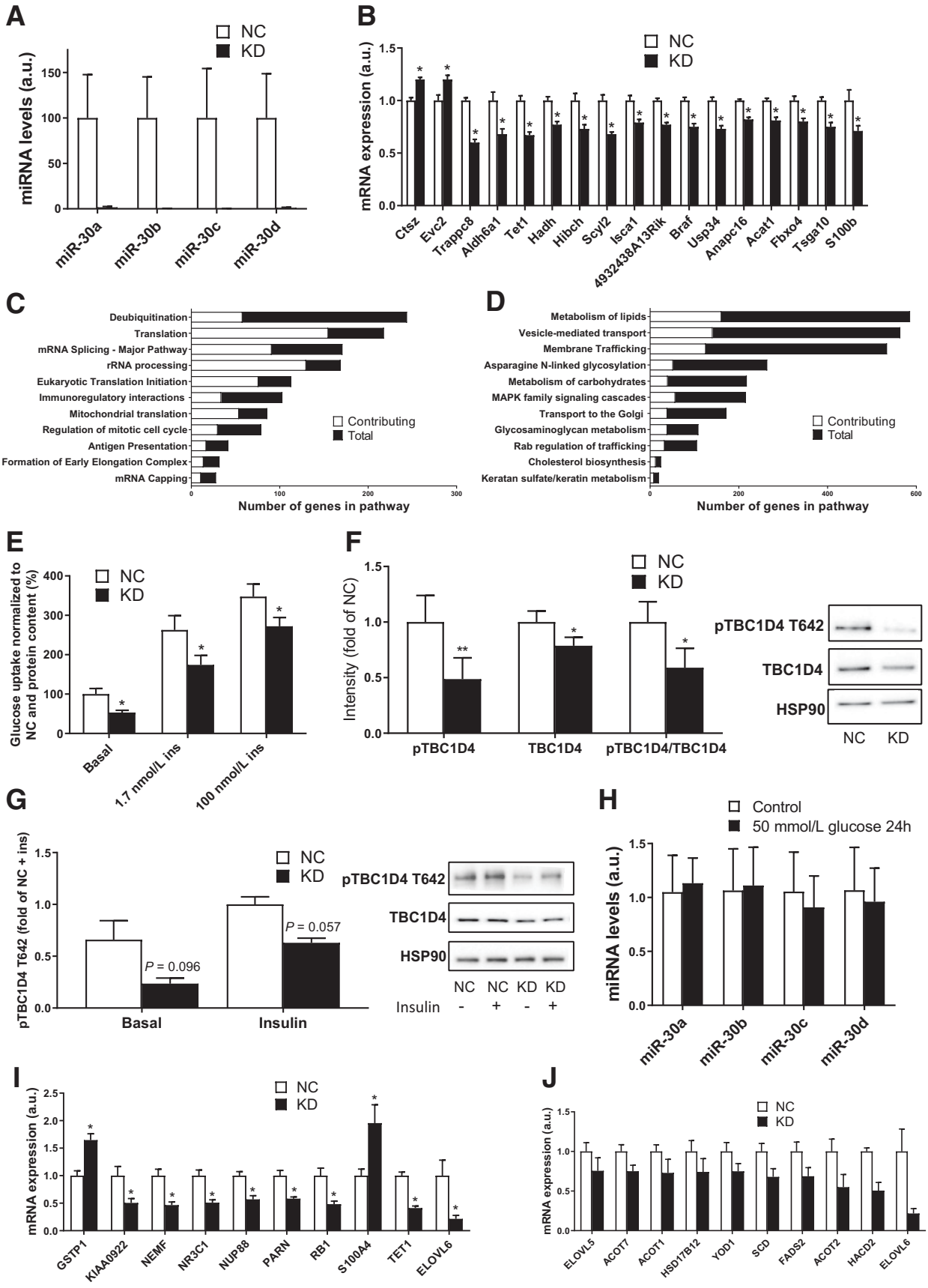

Figure 3—Effect of miR-30 silencing in adipocytes on gene expression, glucose uptake, and insulin signaling. *A*: The expression of miR-30a–d was silenced in mature 3T3-L1 adipocytes by cotransfecting the cells with the mmu-miR-30a-5p and mmu-miR-30c-5p inhibitors (KD). This resulted in KD of the four miRNAs compared with NC: 1.7%, 0.4%, 0.2%, and 1.1% remaining expression, respectively. Data

(Fig. 3*C*). Downregulated pathways included gene sets related to the metabolism of carbohydrates and lipids and to vesicle-mediated transport (Fig. 3*D*).

We analyzed the overlap between differentially expressed genes and in silico predicted miR-30 targets. TargetScan analysis predicted 1,244 conserved targets for the mouse miR-30 family (92.5% matched the predicted targets of the miR-30 family in human). Eight of the predicted target genes were upregulated and 84 were downregulated in miR-30–silenced 3T3-L1 adipocytes ($q < 0.05$) (Supplementary Table 7). Of these, the target gene *Rhebl1* exhibited the largest increase in expression in response to miRNA silencing (log2 FC = 0.67).

Furthermore, we detected 81 downregulated and 14 upregulated transcription factor (TF) genes in silenced adipocytes ($q < 0.05$) (Supplementary Table 8). Expression of *Irf7* encoding the interferon regulatory factor 7 was significantly upregulated (log2 FC = 1.33). The expression of 13 TF genes recognized as conserved predicted targets in mouse by TargetScan was downregulated after silencing, including *PGC1α* (log2 FC = –0.32).

Finally, we used the RcisTarget package (34) (Bioconductor, release 3.10) to search for DNA-binding motifs 5,000 bp upstream and 5,000 bp downstream of the TSS regions of significantly regulated genes in the silenced adipocytes. Indeed, we identified enriched motifs annotated to the IRF family (IRF1, IRF2, IRF4, IRF7, and IRF9) in promoter regions of significantly upregulated genes (Supplementary Table 9). Promoters of the significantly downregulated genes contained enriched motifs associated with ELK4, TAF1, and PHF8 TFs (Supplementary Table 9). Collectively, the data presented above indicate that miR-30 regulates key genes involved in T2D pathology, overlapping with genes differentially expressed in human adipose tissue from T2D versus control subjects.

miR-30 Silencing in 3T3-L1 Adipocytes Affects Glucose Uptake and Insulin Signaling

The increased fasting plasma and 2-h glucose levels (Table 1), the decreased expression of hsa-miR-30a–d (Table 2) in subjects with T2D, and the positive intra–twin pair correlation between hsa-miR-30b and fasting glucose levels (Supplementary Table 1) suggested that the miR-30 family is involved in regulation of glucose metabolism or is regulated by hyperglycemia. We therefore investigated the possible effect of mmu-miR-30a–d silencing on glucose uptake and insulin signaling in 3T3-L1 adipocytes and the effect of 24-h exposure to high glucose concentration on miR-30a, b, c and d levels in these cells. mmu-miR-30 silencing in 3T3-L1 adipocytes resulted in a significantly reduced glucose uptake both in the basal state and in presence of insulin compared with NC ($P < 0.05$) (Fig. 3*E*). There was either no effect (1.7 nmol/L) or an *increase* (100 nmol/L) in the induction of glucose uptake by insulin, i.e., the fold increase compared with the basal, when silencing miR-30 (Supplementary Fig. 8). In search for mechanisms underlying the reduction in glucose uptake, we investigated phosphorylation/activity status of Akt and its substrate TBC1D4—a Rab-GAP whose Akt-mediated phosphorylation is important for GLUT4 translocation to the membrane (35). There was no change in protein levels or phosphorylation of Akt at the activity-controlling site Ser473 after silencing of miR-30 (Supplementary Fig. 9*A* and *B*). However, we found a consistent and marked reduction in total TBC1D4 phosphorylation at the Akt site Thr642 in miR-30–silenced 3T3-L1 adipocytes in the basal state (Fig. 3*F*) and a nominal reduction in the presence of insulin (Fig. 3*G*). We also detected reductions in protein levels and specific phosphorylation (phosphorylation/protein level) of TBC1D4, following miR-30 silencing, although these differences were smaller than for total phosphorylation (Fig. 3*F*). Also, in line with the reduced glucose uptake, mmu-miR-30 silencing resulted in reduced expression of the glucose transporter *Glut1* (*Slc2a1*) ($q < 0.05$) (Supplementary Table 5). However, GLUT1 protein expression was not changed in miR-30–silenced 3T3-L1 adipocytes (Supplementary Fig. 10). Expression of *Glut2*, *3*, and *4* was not affected by miR-30 silencing (Supplementary Table 5).

shown as miRNA levels normalized to snoRNA202 and NC (mean + SEM, $n = 6$). *B*: Seventeen genes that were dysregulated in human T2D adipose tissue, as previously reported (21), were also dysregulated in miR-30–silenced 3T3-L1 adipocytes (*$q < 0.05$ compared with NC, $n = 6$). Data are shown as the mean + SEM, with the NC mean expression levels for all mRNAs set to 1. *C*: Selected pathways with significant enrichment of upregulated genes in response to miR-30 silencing ($q < 0.05$). A complete list of significantly enriched pathways is presented in Supplementary Table 6. *D*: Selected pathways with significant enrichment of downregulated genes in response to miR-30 silencing ($q < 0.05$). A complete list of significantly enriched pathways is presented in Supplementary Table 6. *E*: mmu-miR-30a–d silencing resulted in a significant decrease in the basal and insulin (ins)-stimulated (1.7 nmol/L and 100 nmol/L insulin) glucose uptake in 3T3-L1 cells (*$P < 0.05$ compared with NC, $n = 5$). *F*: There was a reduction in total TBC1D4 phosphorylation (p) at the Akt site Thr642, TBC1D4 protein levels, and specific phosphorylation (phosphorylation/protein level) of TBC1D4 following miR-30 silencing in 3T3-L1 adipocytes. Data are presented as mean + SEM and normalized to HSP90 and NC (*$P < 0.05$ and **$P < 0.01$ compared with NC, $n = 6$). *G*: There was a nominal reduction in total TBC1D4 phosphorylation in the presence of 1 nmol/L insulin following miR-30 silencing in 3T3-L1 adipocytes. Data are presented as mean + SEM and normalized to HSP90 and NC in the presence of insulin ($n = 3$). *H*: Differentiated 3T3-L1 cells (day 10) were cultured for 24 h in either control (25 mmol/L glucose) or elevated (50 mmol/L glucose) glucose DMEM. Direct exposure to high glucose (50 mmol/L) for 24 h did not affect miR-30a, b, c, or d levels in 3T3-L1 adipocytes ($P > 0.05$, $n = 4$ independent experiments). *I*: Ten genes that were dysregulated in human T2D adipose tissue, as previously reported (21), were also dysregulated in the same direction in miR-30–silenced SGBS adipocytes (*$q < 0.05$ compared with NC, $n = 5$). Data are shown as the mean + SD, with the NC mean unlogged expression levels for all mRNAs set to 1. *J*: Genes contributing to the significant enrichment score of GSEA for the "biosynthesis of unsaturated fatty acids" pathway in miR-30 KD SGBS adipocytes vs. NC. Data are shown as the mean + SD, with the NC mean unlogged expression levels for all mRNAs set to 1. a.u., arbitrary units.

Table 4—The 25 most upregulated and 25 most downregulated genes ($q < 0.05$) after mmu-miR-30 silencing in mature 3T3-L1 adipocytes compared with NC

Gene	Entrez Gene identifier	Log2 FC	t	*q*	Regulation	Publication (PMID)
Rtp4	67775	1.774	4.9	0.041	Upregulated	27980621
Mpeg1	17476	1.753	5.16	0.036	Upregulated	29922174
Isg15	100038882	1.695	5.62	0.028	Upregulated	
Bst2	69550	1.647	6.45	0.019	Upregulated	
Apol9a	223672	1.529	6.1	0.022	Upregulated	
Irf7	54123	1.33	4.89	0.041	Upregulated	23695216
Ccl5	20304	1.299	6.92	0.016	Upregulated	31131239
Xaf1	327959	1.291	5.18	0.036	Upregulated	29132171
Phf11d	219132	1.286	5.06	0.038	Upregulated	
Apol9b	71898	1.252	6.39	0.020	Upregulated	
Gbp3	55932	1.25	4.67	0.046	Upregulated	
Ifi27l2a	76933	1.235	11.6	0.004	Upregulated	
Igtp	16145	1.214	5.79	0.026	Upregulated	
Zbp1	58203	1.184	6.92	0.016	Upregulated	
Dhx58	80861	1.052	4.57	0.0498	Upregulated	20973890
Oas1a	246730	1.024	4.68	0.046	Upregulated	
Psmb8	16913	0.965	5.64	0.028	Upregulated	
Gbp11	634650	0.893	5.67	0.027	Upregulated	
Ifit1bl1	667373	0.866	8.62	0.008	Upregulated	
H2-Q4	15015	0.836	8.95	0.007	Upregulated	
Gm8909	667977	0.827	8.02	0.011	Upregulated	
Plac8	231507	0.81	6.11	0.022	Upregulated	26296322
Psmb9	16912	0.805	6.29	0.020	Upregulated	20968039
Cd74	16149	0.784	6.91	0.016	Upregulated	29773671
Slfn2	20556	0.742	5.75	0.026	Upregulated	
Lyrm4	380840	−1.334	−9.06	0.007	Downregulated	
P2ry10b	213438	−1.284	−11.96	0.004	Downregulated	
Chic1	12212	−1.142	−9.67	0.006	Downregulated	
Car5b	56078	−1.129	−16.58	0.003	Downregulated	
AW549877	106064	−1.122	−13.33	0.003	Downregulated	
H60a	15101	−1.093	−6.36	0.020	Downregulated	
Fgf10	14165	−1.056	−13.17	0.003	Downregulated	27412358
Pcna	18538	−1.054	−10.62	0.005	Downregulated	30513216
Pi15	94227	−1.034	−15.3	0.003	Downregulated	
Pqlc3	217430	−1.024	−12.21	0.003	Downregulated	
Prkaa2	108079	−1.015	−6.06	0.023	Downregulated	30646747
Bub1	12235	−0.977	−7.17	0.015	Downregulated	
Sgcd	24052	−0.96	−14.08	0.003	Downregulated	30938105
Peg3	18616	−0.953	−5.61	0.028	Downregulated	27130279
Strn3	94186	−0.946	−15.4	0.003	Downregulated	
Adgrg2	237175	−0.921	−13.9	0.003	Downregulated	
Lum	17022	−0.909	−12.01	0.004	Downregulated	30409703
Slc30a9	109108	−0.895	−8.34	0.009	Downregulated	
Zfp677	210503	−0.874	−13.51	0.003	Downregulated	
Prrg1	546336	−0.874	−10.69	0.005	Downregulated	

Continued on p. 2414

Table 4—Continued

Gene	Entrez Gene identifier	Log2 FC	t	q	Regulation	Publication (PMID)
Olr1	108078	−0.865	−7.2	0.014	Downregulated	
Nectin3	58998	−0.854	−6.43	0.019	Downregulated	
Pank1	75735	−0.851	−5.78	0.026	Downregulated	24781151
Pgap1	241062	−0.842	−5.83	0.025	Downregulated	
Wdsub1	72137	−0.837	−11.16	0.004	Downregulated	

Shown is the association of the genes with T2D, diabetes complications, or obesity in human, animal models, or cells, based on the available literature in PubMed. PMID, PubMed identifier.

Direct exposure of 3T3-L1 adipocytes to high glucose (50 vs. 25 mmol/L glucose) for 24 h had no effect on miR-30a, b, c, or d expression (Fig. 3*H*).

miR-30 Silencing in Human SGBS Adipocytes

We finally tried to validate some of our findings from human T2D adipose tissue and 3T3-L1 miR-30 KD adipocytes in human adipocytes where miR-30 was silenced. Here, we analyzed the transcriptome of miR-30–silenced human SGBS adipocytes using microarray and found 668 significantly downregulated genes ($q < 0.05$) and 249 significantly upregulated genes ($q < 0.05$) compared with NC (Supplementary Table 10). We then studied the overlap of differentially expressed genes ($q < 0.05$) in miR-30–silenced 3T3-L1 versus SGBS adipocytes after conversion of mouse genes to human orthologs (biomaRt package, Bioconductor, release 3.10) and identified 111 common genes regulated in the same direction, which is more than expected by chance ($P < 0.0001$, χ^2 test [marked in Supplementary Table 10]).

We next compared the list of genes with significantly altered expression after miR-30 silencing in SGBS adipocytes (Supplementary Table 10) with the differentially expressed genes in adipose tissue from MZ twins discordant for T2D, where also we discovered reduced miR-30 expression (21) (Fig. 1*A*). This revealed 10 common genes regulated in the same direction including *S100A4*, which was upregulated, as well as *ELOVL6* and *TET1*, which were downregulated, in both data sets (human T2D adipose tissue and SGBS miR-30 KD) (Fig. 3*I*). Notably, S100A4 was recently identified as a novel adipokine associated with insulin resistance and inflammation/adipocyte hypertrophy (36). We then used GSEA to identify sets of biologically related genes that are altered in both the miR-30–silenced human adipocytes and in human T2D adipose tissue. GSEA revealed that the pathway "biosynthesis of unsaturated fatty acids" is downregulated in both SGBS miR-30 KD and twins with T2D (21) (Fig. 3*J* and Supplementary Table 11).

Next, we analyzed the overlap between differentially expressed genes in miR-30–silenced SGBS adipocytes and in silico predicted miR-30 targets. TargetScan analysis predicted 1,576 conserved targets for the human miR-30 family. Fifteen of the predicted target genes were upregulated and 117 were downregulated in miR-30–silenced SGBS adipocytes ($q < 0.05$) (Supplementary Table 12). Twenty-four target genes were differentially expressed in both miR-30–silenced 3T3-L1 adipocytes and SGBS adipocytes (marked in Supplementary Table 12). Interestingly, *TET1* and *ELOVL6* were downregulated in SGBS miR-30 KD adipocytes and human T2D adipose tissue and are conserved predicted targets of the human miR-30 family. In line with this, there was a trend toward lower ELOVL6 protein levels in SGBS adipocytes after miR-30 silencing (Supplementary Fig. 11).

DISCUSSION

The role of miRNAs in the pathology of T2D and their potential as therapeutic targets remain to be explored adequately. In this study, we identified a set of miRNAs that were differentially expressed in T2D by using adipose tissue from two human cohorts. We were able to demonstrate the potential regulation of miRNA expression by DNA methylation and the physiological consequences of miRNA level dysregulation, reminiscent of the T2D pathology, in vitro (Fig. 4).

We identified 25 miRNAs as downregulated and 5 as upregulated in twins with T2D compared with their corresponding co-twins without T2D. The hsa-miR-30 and hsa-let-7 families were overrepresented among the dysregulated miRNAs in discordant twins, with four members of each family downregulated in T2D individuals, a finding confirmed in the case-control cohort. The coordinated behavior of miRNAs belonging to the same family and, thus, targeting the same mRNAs is thought to strengthen their concerted effect on gene regulation. The miR-30 and let-7 family members have previously been shown to be associated with T2D pathology, as they affect adipogenesis, glucose metabolism, and inflammatory processes (37–40). For example, hsa-miR-30e and hsa-let-7i were shown to be downregulated in muscle from MZ twins with T2D compared with their co-twins without diabetes (19). Additionally, mir-30a, miR-30c, and miR-30e were downregulated in adipose tissue macrophages of mouse fed a high-fat diet, affecting Notch1 signaling and proinflammatory cytokine production (41).

Our previous analysis of mRNA expression in adipose tissue from MZ twins discordant for T2D (21) revealed

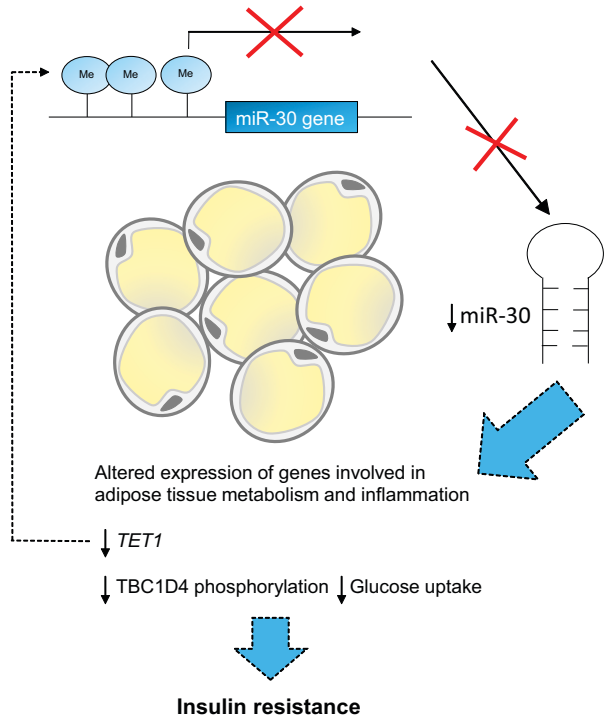

Figure 4—Proposed model of miR-30 regulation and activity in adipose tissue, and the potential role in the development of insulin resistance. As shown in the current study, miR-30 levels are reduced in adipose tissue of subjects with T2D. Concurrently, methylation of the promoter of *miR-30a* was increased in T2D subjects in the two cohorts analyzed. Increased methylation of the *miR-30a* promoter reduced the transcriptional activity of this miRNA gene in vitro and could therefore be one mechanism behind the dysregulation. Further, silencing of miR-30 in adipocytes resulted in reduced glucose uptake and TBC1D4 phosphorylation, downregulation of genes involved in carbohydrate/lipid/amino acid metabolism, and upregulation of genes related to the immune system. These changes could eventually result in insulin resistance. At present, the factors that lead to differential methylation of miRNA gene promoters in T2D are not known, but we speculate that the reduced expression of *TET1* seen in human T2D adipose tissue and 3T3-L1/SGBS adipocytes lacking miR-30 could be one such factor. The gaps require further investigation in future studies.

decreased expression of energy metabolism genes and increased expression of inflammatory genes in subjects with T2D. Based on the findings of the current study, we speculate that altered miRNA levels in T2D subjects could underpin this expression pattern. To investigate this further we therefore performed experiments where we silenced miRNAs in cultured adipocytes. The main part of these experiments was performed in the well-characterized mouse 3T3-L1 cell line, in which protocols for gene silencing and the study of insulin action were already established. However, we also used the SGBS cell strain to validate our results in cells of human origin. Indeed, silencing of the miR-30 family in cultured adipoctes affected expression of almost 1,000 genes, with dysregulated genes related to glucose and lipid metabolism, and the immune system, similar to the pattern seen in adipose tissue from T2D subjects. This suggests that the downregulation of miR-30 in T2D subjects can, at least partially, be responsible for changes observed in human T2D adipose tissue. miRNA regulatory networks are enormously complex because hundreds of miRNAs might target one mRNA, either directly or indirectly, e.g., through TFs. In fact, we detected nearly 100 up- or downregulated genes encoding TFs in miR-30–silenced 3T3-L1 adipocytes. *Irf7* is of particular interest among the upregulated TF genes: it is a predicted miR-30 target, and the promoter regions of significantly upregulated genes in miR-30–silenced adipocytes are enriched with TF-binding motifs annotated with the IRF family. Moreover, IRFs are recognized transcriptional regulators of adipogenesis (42).

Analysis of overlapping genes in the adipose tissue mRNA data set from T2D discordant twins and 3T3-L1 adipocytes lacking miR-30a–d revealed genes related to fatty acid or amino acid metabolism with links to T2D and/or adipocytes, including *HADH*, *ACAT1*, *ALDH6A1*, and *HIBCH*. Notably, downregulation of the genes encoding acetyl-CoA acetyltransferase 1 (*ACAT1*) and aldehyde dehydrogenase 6 family, member A1 (*ALDH6A1*), has previously been observed in adipose tissue from obese T2D patients (43). Analysis of overlapping genes in the adipose tissue mRNA data set from T2D discordant twins and human SGBS adipocytes lacking miR-30a–d also revealed genes related to fatty acid metabolism with links to T2D and/or adipocytes. In particular, *ELOVL6*, encoding a key enzyme in the elongation of long-chain fatty acids, was downregulated in both T2D subjects and miR-30–silenced SGBS adipocytes.

We detected only a small overlap between the in silico predicted targets and significantly upregulated genes in miR-30–silenced adipocytes. This could indicate a primary involvement of miR-30 in posttranscriptional regulation, with a minor effect on mRNA levels, or the fact that not all mRNA targets are expressed in adipocytes. This could also be a matter of timing, since some mRNAs might be degraded only after an initial inhibition of translation (44). Interestingly, more genes were significantly downregulated than upregulated in miR-30–silenced adipocytes. According to previous studies, silencing of a miRNA leads to both up- and downregulation of mRNA and protein levels, suggesting that the ability of miRNAs to upregulate mRNA and protein levels may be more common than currently appreciated. Upregulation may, for example, be a result of the miRNA blocking the binding of repressing factors to mRNA (45), or it could be caused by competition of multiple miRNAs for the same mRNA target (46).

Although changes in miRNA expression have been demonstrated in various diseases, knowledge of the underlying mechanisms is limited. miRNA biogenesis is regulated on multiple levels, including transcription, processing, and editing. A link between epigenetic changes and miRNAs has been described for several physiological processes, and miRNA expression can be downregulated by methylation of the promoter (8–12). In the current study we demonstrated, for the first time, the association

of differential DNA methylation with altered miRNA expression in adipose tissue from subjects with T2D. Methylation of five sites annotated to differentially expressed miRNAs was increased in adipose tissue from T2D subjects in the two cohorts analyzed, including sites in the promoters of *hsa-miR-30a* and *hsa- let-7a-3*. In this study we analyzed DNA methylation using the Illumina Infinium HumanMethylation450 array. Importantly, we have previously both technically and biologically validated DNA methylation data generated using this array in several human cohorts via other methods (9,47). Further, the luciferase reporter experiments confirmed that methylation of the *hsa-miR-30a* promoter suppresses expression of that gene. This is in line with another study where *miR-30a* promoter hypermethylation correlated with reduced expression (48). DNA hypermethylation in the promoter and decreased hsa-let-7a-3 expression have been observed in blood from patients with diabetic nephropathy (49). Methylation of the *hsa-let-7a-3* promoter in the luciferase experiments in our study nominally suppressed the miRNA expression, although the effect was not statistically significant. This suggests that DNA methylation might be one, but not the sole, mechanism regulating let-7 levels. For instance, the long noncoding RNA H19 is an important regulator of the let-7 family (50). Additional epigenetic mechanisms, such as histone modifications, may also play a role in miRNA expression regulation, which should be investigated in future studies.

Differentially expressed miRNAs could be an effect and/or a cause of metabolic imbalance. It is important to distinguish the primary mechanisms relevant to development of T2D from secondary changes caused by the disease. The observations of dysregulated miRNAs in T2D adipose tissue and intra–twin pair correlations between differences in fasting glucose and miRNA levels suggest that these miRNAs are either involved in regulation of glucose metabolism or are regulated by hyperglycemia as an effect secondary to T2D. Accordingly, we focused on the miR-30 family to investigate its potential role in adipocyte glucose metabolism in detail. Downregulation of miR-30 in adipocytes resulted in decreased glucose uptake in the basal state and to a lesser extent in the presence of insulin. In line with this, miR-30 silencing reduced phosphorylation of TBC1D4, which in its unphosphorylated form contributes to anchoring of GLUT4-containing vesicles in the cytosol (35). Notably, another study found lower TBC1D4 phosphorylation in adipose tissue from T2D subjects versus subjects without diabetes (51). As for glucose uptake, phosphorylation of TBC1D4 was in our study markedly reduced in the basal state and slightly less so in the presence of insulin. The mechanism underlying reduced TBC1D4 phosphorylation does not appear to involve changes in Akt activity, as Akt expression and phosphorylation were unaffected by miR-30 silencing. Direct exposure of 3T3-L1 adipocytes to high glucose did not affect miR-30 expression, suggesting that the reduced miR-30 expression in T2D adipose tissue is not caused by hyperglycemia.

The current study has some limitations. First, although the concept of MZ twin pairs discordant for T2D makes for a powerful study design, these twins are rare and the relatively small sample size increases the risk of type II errors. Additional dysregulated miRNAs might have been identified in a larger cohort. However, the performed validation in an independent case-control cohort supports the biological relevance of the presented findings in relation to T2D. Further, it is well established that the methylome is heritable (21,52–54), and this may explain why we identified more DNA methylation differences in unrelated subjects from the case-control cohort than in the MZ discordant twins.

Understanding the miRNA-guided network of gene expression regulation can potentially provide new tools for the diagnosis and therapy of many human diseases. Several years ago, the miR-34a mimic MRX34, a master regulator of tumor suppression, was the first miRNA mimic to reach phase 1 studies (55). Recent data suggest that miRNAs may constitute attractive therapeutic targets for T2D too by improving β-cell function (14) or insulin sensitivity (15), and our findings help substantiate this statement. In the future, in vivo delivery of miRNA mimics or anti-miRNAs specifically in insulin target tissues could permit correcting the level of key miRNAs under diabetes conditions and lead to new strategies for treating the disease.

Acknowledgments. The authors thank Swegene Center for Integrative Biology at Lund University (SCIBLU) genomics facility for help with global DNA methylation and miRNA and mRNA expression analyses as well as the Bioinformatics and Expression Analysis core facility at Karolinska Institute for help with mRNA expression analyses. The authors thank Jette Bork-Jensen (University of Copenhagen, Copenhagen, Denmark) for valuable miRNA discussions, Martin Wabitsch (University of Ulm, Ulm, Germany) for providing the SGBS cell line, and Kasper Pilgaard for excision of human adipose tissue from three individuals with T2D and three control subjects at Steno Diabetes Center Copenhagen. The authors thank the Nordic Network for Clinical Islet Transplantation (JDRF award 31-2008-413) and the tissue isolation teams and Human Tissue Laboratory within EXODIAB/Lund University Diabetes Centre for providing human adipose tissue from 5 individuals with T2D and 10 control subjects.

Funding. This work was supported by the Swedish Research Council (grants Dnr 2016-02486, 2018-02567, and 2019-01406 and Strategic Research Area Exodiab Dnr 2009-1039), Region Skåne and ALF, the Novo Nordisk Foundation, the Swedish Foundation for Strategic Research (Dnr IRC15-0067), the Syskonen Svensson Foundation, the Diabetes Foundation, Kungliga Fysiografiska Sällskapet i Lund, Magnus Bergvall Foundation, Åke Wiberg Foundation, the European Foundation for the Study of Diabetes/Lilly Programme, the Söderberg Foundation, and the Påhlsson Foundation. The Swedish twins were recruited from the Swedish Twin Registry, which is supported by grants from the Swedish Department of Higher Education and the Swedish Research Council.

Duality of Interest. No potential conflicts of interest relevant to this article were reported.

Author Contributions. E.N. and C.L. designed the study, researched data, and wrote the manuscript. M.V. performed in vitro experiments, analyzed data, and wrote the manuscript. J.S. performed in vitro experiments and analyzed data. A.P. analyzed data. P.-A.J. and P.P. collected the clinical material and data. J.L.S.E., L.E., and O.G. supervised and contributed to the experimental design. A.V. contributed to study design and collected the clinical material and data. All authors reviewed and approved the final version of the manuscript. E.N. is the guarantor of this work and, as such, had full access to all the data in the study and takes responsibility for the integrity of the data and the accuracy of the data analysis.

References

1. Petersen MC, Shulman GI. Mechanisms of insulin action and insulin resistance. Physiol Rev 2018;98:2133–2223
2. Jackson RA, Roshania RD, Hawa MI, Sim BM, DiSilvio L. Impact of glucose ingestion on hepatic and peripheral glucose metabolism in man: an analysis based on simultaneous use of the forearm and double isotope techniques. J Clin Endocrinol Metab 1986;63:541–549
3. Abel ED, Peroni O, Kim JK, et al. Adipose-selective targeting of the GLUT4 gene impairs insulin action in muscle and liver. Nature 2001;409:729–733
4. McGregor RA, Choi MS. microRNAs in the regulation of adipogenesis and obesity. Curr Mol Med 2011;11:304–316
5. Qin L, Chen Y, Niu Y, et al. A deep investigation into the adipogenesis mechanism: profile of microRNAs regulating adipogenesis by modulating the canonical Wnt/beta-catenin signaling pathway. BMC Genomics 2010; 11:320
6. Xu G, Ji C, Song G, et al. MiR-26b modulates insulin sensitivity in adipocytes by interrupting the PTEN/PI3K/AKT pathway. Int J Obes 2015;39:1523–1530
7. Martinelli R, Nardelli C, Pilone V, et al. miR-519d overexpression is associated with human obesity. Obesity (Silver Spring) 2010;18:2170–2176
8. Chhabra R. miRNA and methylation: a multifaceted liaison. ChemBioChem 2015;16:195–203
9. Hall E, Volkov P, Dayeh T, et al. Sex differences in the genome-wide DNA methylation pattern and impact on gene expression, microRNA levels and insulin secretion in human pancreatic islets. Genome Biol 2014;15:522
10. Pan P, Weisenberger DJ, Zheng S, et al. Aberrant DNA methylation of miRNAs in Fuchs endothelial corneal dystrophy. Sci Rep 2019;9:16385
11. Huang YW, Liu JC, Deatherage DE, et al. Epigenetic repression of microRNA-129-2 leads to overexpression of SOX4 oncogene in endometrial cancer. Cancer Res 2009;69:9038–9046
12. Lujambio A, Ropero S, Ballestar E, et al. Genetic unmasking of an epigenetically silenced microRNA in human cancer cells. Cancer Res 2007;67:1424–1429
13. Ferland-McCollough D, Fernandez-Twinn DS, Cannell IG, et al. Programming of adipose tissue miR-483-3p and GDF-3 expression by maternal diet in type 2 diabetes. Cell Death Differ 2012;19:1003–1012
14. Bijkerk R, Esguerra JLS, Ellenbroek JH, et al. In vivo silencing of microRNA-132 reduces blood glucose and improves insulin secretion. Nucleic Acid Ther 2019;29:67–72
15. Trajkovski M, Hausser J, Soutschek J, et al. MicroRNAs 103 and 107 regulate insulin sensitivity. Nature 2011;474:649–653
16. Arner P, Kulyté A. MicroRNA regulatory networks in human adipose tissue and obesity. Nat Rev Endocrinol 2015;11:276–288
17. Dahlman I, Belarbi Y, Laurencikiene J, Pettersson AM, Arner P, Kulyté A. Comprehensive functional screening of miRNAs involved in fat cell insulin sensitivity among women. Am J Physiol Endocrinol Metab 2017;312:E482–E494
18. Bork-Jensen J, Thuesen AC, Bang-Bertelsen CH, et al. Genetic versus non-genetic regulation of miR-103, miR-143 and miR-483-3p expression in adipose tissue and their metabolic implications-a twin study. Genes (Basel) 2014;5:508–517
19. Bork-Jensen J, Scheele C, Christophersen DV, et al. Glucose tolerance is associated with differential expression of microRNAs in skeletal muscle: results from studies of twins with and without type 2 diabetes. Diabetologia 2015;58:363–373
20. Poulsen P, Grunnet LG, Pilgaard K, et al. Increased risk of type 2 diabetes in elderly twins. Diabetes 2009;58:1350–1355
21. Nilsson E, Jansson PA, Perfilyev A, et al. Altered DNA methylation and differential expression of genes influencing metabolism and inflammation in adipose tissue from subjects with type 2 diabetes. Diabetes 2014;63:2962–2976
22. Bolstad BM, Irizarry RA, Astrand M, Speed TP. A comparison of normalization methods for high density oligonucleotide array data based on variance and bias. Bioinformatics 2003;19:185–193
23. Civelek M, Hagopian R, Pan C, et al. Genetic regulation of human adipose microRNA expression and its consequences for metabolic traits. Hum Mol Genet 2013;22:3023–3037
24. Parts L, Hedman AK, Keildson S, et al.; MuTHER Consortium. Extent, causes, and consequences of small RNA expression variation in human adipose tissue. PLoS Genet 2012;8:e1002704
25. Ritchie ME, Phipson B, Wu D, et al. limma powers differential expression analyses for RNA-sequencing and microarray studies. Nucleic Acids Res 2015;43:e47
26. Fabregat A, Jupe S, Matthews L, et al. The Reactome Pathway Knowledgebase. Nucleic Acids Res 2018;46:D649–D655
27. Hajduch E, Alessi DR, Hemmings BA, Hundal HS. Constitutive activation of protein kinase B alpha by membrane targeting promotes glucose and system A amino acid transport, protein synthesis, and inactivation of glycogen synthase kinase 3 in L6 muscle cells. Diabetes 1998;47:1006–1013
28. Bradford MM. A rapid and sensitive method for the quantitation of microgram quantities of protein utilizing the principle of protein-dye binding. Anal Biochem 1976;72:248–254
29. Fischer-Posovszky P, Newell FS, Wabitsch M, Tornqvist HE. Human SGBS cells - a unique tool for studies of human fat cell biology. Obes Facts 2008; 1:184–189
30. Subramanian A, Tamayo P, Mootha VK, et al. Gene set enrichment analysis: a knowledge-based approach for interpreting genome-wide expression profiles. Proc Natl Acad Sci U S A 2005;102:15545–15550
31. Kozomara A, Griffiths-Jones S. miRBase: annotating high confidence microRNAs using deep sequencing data. Nucleic Acids Res 2014;42: D68–D73
32. Agarwal V, Bell GW, Nam JW, Bartel DP. Predicting effective microRNA target sites in mammalian mRNAs. eLife 2015;4:e05005
33. Nägler DK, Lechner AM, Oettl A, et al. An enzyme-linked immunosorbent assay for human cathepsin X, a potential new inflammatory marker. J Immunol Methods 2006;308:241–250
34. Aibar S, González-Blas CB, Moerman T, et al. SCENIC: single-cell regulatory network inference and clustering. Nat Methods 2017;14:1083–1086
35. Sakamoto K, Holman GD. Emerging role for AS160/TBC1D4 and TBC1D1 in the regulation of GLUT4 traffic. Am J Physiol Endocrinol Metab 2008;295:E29–E37
36. Arner P, Petrus P, Esteve D, et al. Screening of potential adipokines identifies S100A4 as a marker of pernicious adipose tissue and insulin resistance. Int J Obes 2018;42:2047–2056
37. Arner E, Mejhert N, Kulyté A, et al. Adipose tissue microRNAs as regulators of CCL2 production in human obesity. Diabetes 2012;61:1986–1993
38. Frost RJ, Olson EN. Control of glucose homeostasis and insulin sensitivity by the Let-7 family of microRNAs. Proc Natl Acad Sci USA 2011;108: 21075–21080
39. Koh EH, Chernis N, Saha PK, et al. miR-30a remodels subcutaneous adipose tissue inflammation to improve insulin sensitivity in obesity. Diabetes 2018;67:2541–2553

40. Zaragosi LE, Wdziekonski B, Brigand KL, et al. Small RNA sequencing reveals miR-642a-3p as a novel adipocyte-specific microRNA and miR-30 as a key regulator of human adipogenesis. Genome Biol 2011;12:R64
41. Miranda K, Yang X, Bam M, Murphy EA, Nagarkatti PS, Nagarkatti M. MicroRNA-30 modulates metabolic inflammation by regulating Notch signaling in adipose tissue macrophages. Int J Obes 2018;42:1140–1150
42. Eguchi J, Yan QW, Schones DE, et al. Interferon regulatory factors are transcriptional regulators of adipogenesis. Cell Metab 2008;7:86–94
43. Dharuri H, 't Hoen PA, van Klinken JB, et al. Downregulation of the acetyl-CoA metabolic network in adipose tissue of obese diabetic individuals and recovery after weight loss. Diabetologia 2014;57:2384–2392
44. Selbach M, Schwanhäusser B, Thierfelder N, Fang Z, Khanin R, Rajewsky N. Widespread changes in protein synthesis induced by microRNAs. Nature 2008;455:58–63
45. Cordes KR, Srivastava D. MicroRNA regulation of cardiovascular development. Circ Res 2009;104:724–732
46. Nyayanit D, Gadgil CJ. Mathematical modeling of combinatorial regulation suggests that apparent positive regulation of targets by miRNA could be an artifact resulting from competition for mRNA. RNA 2015;21:307–319
47. Rönn T, Volkov P, Davegårdh C, et al. A six months exercise intervention influences the genome-wide DNA methylation pattern in human adipose tissue. PLoS Genet 2013;9:e1003572
48. Saleh AD, Cheng H, Martin SE, et al. Integrated genomic and functional microRNA analysis identifies miR-30-5p as a tumor suppressor and potential therapeutic nanomedicine in head and neck cancer. Clin Cancer Res 2019;25:2860–2873
49. Peng R, Liu H, Peng H, et al. Promoter hypermethylation of let-7a-3 is relevant to its down-expression in diabetic nephropathy by targeting UHRF1. Gene 2015;570:57–63
50. Kallen AN, Zhou XB, Xu J, et al. The imprinted H19 lncRNA antagonizes let-7 microRNAs. Mol Cell 2013;52:101–112
51. Stafeev IS, Sklyanik IA, Yah'yaev KA, et al. Low AS160 and high SGK basal phosphorylation associates with impaired incretin profile and type 2 diabetes in adipose tissue of obese patients. Diabetes Res Clin Pract 2019; 158:107928
52. Grundberg E, Meduri E, Sandling JK, et al.; Multiple Tissue Human Expression Resource Consortium. Global analysis of DNA methylation variation in adipose tissue from twins reveals links to disease-associated variants in distal regulatory elements. Am J Hum Genet 2013;93:876–890
53. Ribel-Madsen R, Fraga MF, Jacobsen S, et al. Genome-wide analysis of DNA methylation differences in muscle and fat from monozygotic twins discordant for type 2 diabetes. PLoS One 2012;7:e51302
54. Volkov P, Olsson AH, Gillberg L, et al. A genome-wide mQTL analysis in human adipose tissue identifies genetic variants associated with DNA methylation, gene expression and metabolic traits. PLoS One 2016;11: e0157776
55. Bouchie A. First microRNA mimic enters clinic. Nat Biotechnol 2013; 31:577